

Received 10 December 2019; accepted 21 December 2019. Date of publication 24 December 2019; date of current version 10 January 2020.  
The review of this article was arranged by Editor C. C. McAndrew.

Digital Object Identifier 10.1109/JEDS.2019.2962007

# An Analytical Breakdown Model for the SOI LDMOS With Arbitrary Drift Doping Profile by Using Effective Substrate Voltage Method

KEMENG YANG<sup>1,2,3</sup> (Student Member, IEEE), YUFENG GUO<sup>1,2,3</sup> (Member, IEEE),  
JUN ZHANG<sup>1,2,3</sup> (Member, IEEE), JIAFEI YAO<sup>1,2,3</sup> (Member, IEEE), MAN LI<sup>1,2,3</sup>,  
LING DU<sup>1,2,3</sup>, AND XIAOMING HUANG<sup>1,2,3</sup>

<sup>1</sup> College of Electronic and Optical Engineering, Nanjing University of Posts and Telecommunications; Nanjing 210003, China

<sup>2</sup> College of Microelectronics, Nanjing University of Posts and Telecommunications; Nanjing 210003, China

<sup>3</sup> National and Local Joint Engineering Laboratory of RF Integration and Micro-Assembly Technology, Nanjing University of Posts and Telecommunications, Nanjing 210003, China

CORRESPONDING AUTHOR: Y. GUO (e-mail: yfguo@njupt.edu.cn)

This work was supported by the National Natural Science Foundation of China under Grant 61874059, Grant 61704084, and Grant 61574081.

**ABSTRACT** To elaborate on the relationship between sophisticated 2-D doping profile of drift region and device's breakdown behavior, a unified analytical model for the SOI LDMOS is developed in this paper. The Effective Substrate Voltage (ESV) concept is proposed so that the derivation of electric field and breakdown voltage can be simplified significantly. The ESV indicates that the influence of 2-D doping in the drift region can be equivalent to a virtual substrate potential. By using the proposed model, the role of 2-D drift doping, both continuous or discrete doping profile, in SOI LDMOSs' off-state breakdown behavior is investigated along with the TCAD simulations and experimental results. The good agreement between the analytical, measured and simulated results validates the accuracy of the developed model. A unified RESURF criterion is derived to idealize the electric field in the drift region and therefore maximize the breakdown voltage by optimizing the lateral and vertical drift doping profiles and geometric parameters. The proposed approach provides a universally applicable tool to explore the breakdown mechanism of SOI LDMOS with various drift doping profiles.

**INDEX TERMS** LDMOS, arbitrary doping profile, electric field, breakdown voltage (BV).

## I. INTRODUCTION

Breakdown voltage and on-resistance are critical performances for the lateral power devices, such as Lateral Double-diffused MOSFET (LDMOS) [1]–[4]. Many techniques have been proposed to obtain a better trade-off between BV and  $R_{on}$  by optimizing the drift doping profile. Among them, the most direct and commonly used approaches optimize the lateral breakdown characteristic via altering lateral doping profile, such as the Variation of Lateral Doping (VLD), Single/Double/Triple Reduced Surface Field (RESURF) (S/D/T-RESURF), and Lateral Step Doping (LSD) techniques [5]–[13]. However, due to the limitation of actual process or the requirement of design, the vertical doping profile can hardly be uniform. In fact, the vertical doping profile of the drift region also plays a significant

role in affecting the devices' BV and  $R_{on}$  performances. In practice, Gaussian doping and linear doping is most commonly seen profile in the vertical direction, the devices' breakdown characteristics are sensitive to the diffusion time as the diffusion time influences the vertical doping profile of the drift region. Unfortunately, present models are usually derived based on the assumption of a uniform vertical doping profile [14]–[17]. For instance, although the novel and delicate method uses Green's Function in modeling VLD devices, the variation of the vertical doping profile is not considered in this derivation [17]–[20]. Thus, the impact of variation in the vertical doping profile on the electric field of power devices can not be discussed using these models. In terms of the device with variation of vertical doping profile, [6] gives a method to model this device based on the

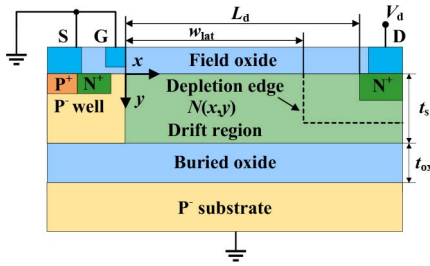


**FIGURE 1.** 2-D cross section of the SOI LDMOS with an arbitrary doping profile in the drift region.

assumption that doping profile of each small layer is uniform. However, such a method still incapable of considering the variation of lateral and vertical doping profiles simultaneously as a result of the derivation complexity of which method. The missing of a practical analytical methodology for lateral power devices with arbitrary drift doping profile makes the optimized devices often perform a degraded breakdown characteristic [17].

To explore the mechanism of off-state breakdown performance in SOI LDMOS with arbitrary drift doping profiles, a unified analytical breakdown model is developed via using the effective substrate voltage concept. Therefore, the derivation of 2D Poisson's equation can be greatly simplified. A universally applicable analytical model is obtained accordingly. By using which, devices with continuous and discrete doping profiles are analyzed. The analytical results agree well with results measured by [8], [9] and results simulated by MEDICI, a commercial TCAD tool. The simulation models used in MEDICI are CONSRH, AUGER, BGN, FLDMOB, IMPACT. I and CCSMOB. This agreement verifies that the proposed model has a wide range of applications. Furthermore, based on the derived models, a RESURF criterion is obtained to achieve an ideal surface electric field in devices.

## II. SURFACE ELECTRIC FIELD

### A. METHOD OF EFFECTIVE SUBSTRATE VOLTAGE

The doping profile influences the breakdown characteristics of the lateral power devices. However, the model in [6] and [17] can only depict the influence of variation of vertical or lateral doping profile, separately. To give a clear breakdown mechanism of SOI LDMOS with arbitrary drift doping profiles, in this part, the method of effective substrate voltage is proposed to simplify the equations and avoid the complex derivation in [6].

The cross-section of the SOI LDMOS with an arbitrary doping profile in the drift region is shown in Fig. 1.  $N(x, y)$  represents the doping concentration of the drift region which varies in both the  $x$  and  $y$  directions.  $L_d$  is the length of the drift region. The lateral depletion width is denoted as  $w_{lat}$ .  $t_s$  and  $t_{ox}$  are the thicknesses of the drift region and buried oxide, respectively.

When the drift region is fully depleted at a given reversed biased voltage  $V_d$ , the surface electric potential  $\varphi(x, y)$  in

silicon film satisfies the 2-D Poisson's equation and boundary conditions, which can be given by:

$$\frac{\partial^2 \varphi(x, y)}{\partial x^2} + \frac{\partial^2 \varphi(x, y)}{\partial y^2} = -\frac{qN(x, y)}{\epsilon_s} \quad (1)$$

$$\varphi(0, 0) = 0, \varphi(L_d, 0) = V_d \quad (2)$$

$$\frac{\partial \varphi(x, y)}{\partial y} \Big|_{y=0} = 0, \frac{\partial \varphi(x, y)}{\partial y} \Big|_{y=t_s} = -\frac{\varphi(x, t_s)}{\epsilon_s t_{ox} / \epsilon_{ox}} \quad (3)$$

where  $q$  is the elementary charge, and  $\epsilon_s$  and  $\epsilon_{ox}$  are the dielectric constant of silicon and silicon oxide materials, respectively. The boundary condition Eq. (3) is based on the continuity of electric flux density across the front and back Si/SiO<sub>2</sub> interfaces. Fig. 2 gives the method of effective substrate voltage to simplify the equation. The potential and electric field of the drift region is caused by the applied voltage and drift doping profile, as shown in Fig. 2(a)-(c). The potential and electric field, including the lateral and vertical electric field, induced by the depleted drift impurities can be equivalent to the variation of an effective substrate voltage. To obtain this effective substrate voltage, the differential layer  $dy$  and the substrate are considered as plates of the differential capacitance, as shown in Fig. 2(d). The charge and value of this capacitance yield as follows:

$$dQ(x, y) = qN(x, y)dy \quad (4)$$

$$C_T(y) = \frac{\epsilon_s}{t_s + \epsilon_{ox} t_{ox} / \epsilon_s - y} \quad (5)$$

Fig. 2(e) reveals that the electric field of the differential layer can be replaced by the differential effective substrate voltage. The total effective substrate voltage is obtained by integrating the differential effective substrate voltage, yielded as:

$$\begin{aligned} V_0(x) &= \int_0^{t_s} \frac{dQ(x, y)}{C_T(y)} \\ &= \frac{q}{\epsilon_s} \int_0^{t_s} (t_s + \epsilon_{ox} t_{ox} / \epsilon_s - y) N(x, y) dy \end{aligned} \quad (6)$$

As the effective substrate voltage  $V_0$  is applied, the non-uniform drift doping profile in Fig. 2 (a) can be replaced by the intrinsic drift region in Fig. 2 (g). Poisson's equation Eq. (1) and the boundary condition Eq. (3) can be transformed into:

$$\frac{\partial^2 \varphi(x, y)}{\partial x^2} + \frac{\partial^2 \varphi(x, y)}{\partial y^2} = 0 \quad (7)$$

$$\frac{\partial \varphi(x, y)}{\partial y} \Big|_{y=0} = 0, \frac{\partial \varphi(x, y)}{\partial y} \Big|_{y=t_s} = \frac{V_0(x) - \varphi(x, t_s)}{\epsilon_s t_{ox} / \epsilon_{ox}} \quad (8)$$

The potential function can be approximated to a quadratic function of  $y$ , which yields [6], [16]

$$\varphi(x, y) \approx \varphi(x, 0) + \varphi_1(x)y + \varphi_2(x)y^2 \quad (9)$$

Substituting Eq. (8)-(9) into Eq. (7), the 2-D Laplace equation can be transformed into:

$$\frac{d^2 \varphi(x, 0)}{dx^2} - \frac{\varphi(x, 0)}{t^2} = -\frac{V_0(x)}{t^2} \quad (10)$$

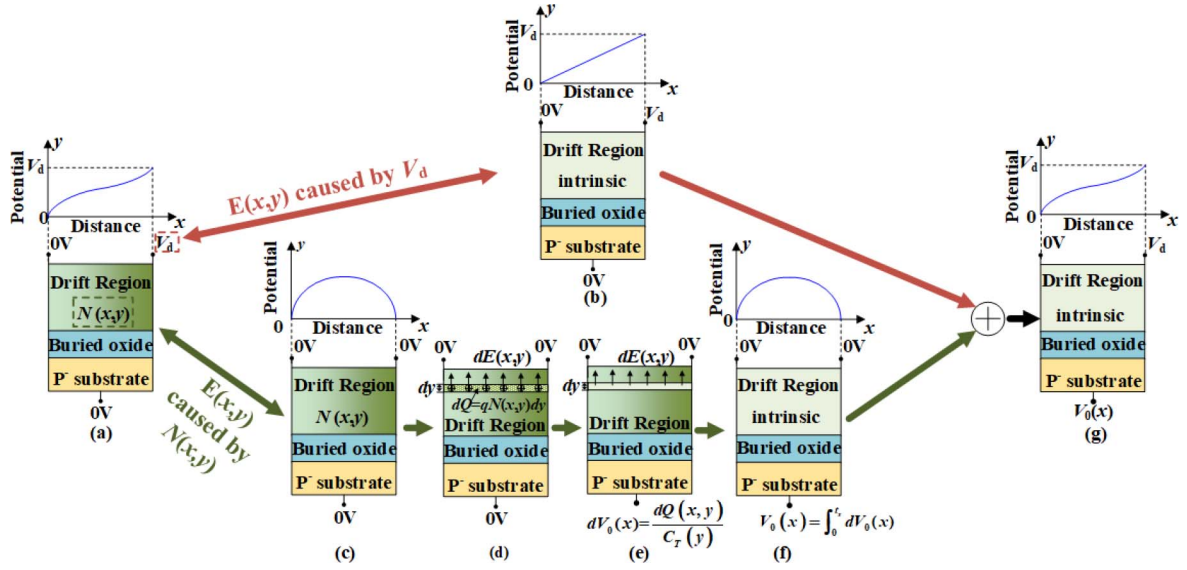


**FIGURE 2.** Method of equivalent substrate voltage: schematic of (a) device with applied drain voltage and its surface potential; (b) potential caused by applied voltage; (c) potential caused by depleted charges; (d) electric field caused by the differential layer; (e) electric field replaced by the differential effective substrate voltage; (f) method to calculate effective substrate voltage; (g) equivalent device with effective substrate voltage and its surface potential.

where  $t = (0.5t_s^2 + t_s t_{ox} \epsilon_s / \epsilon_{ox})^{0.5}$  is the characteristic thickness. Due to the reduction in the dimension of the Poisson's equation, the boundary condition at left and right of the drift region is not required here. By submitting boundary condition Eq. (2) into Eq. (10), the surface potential and electric field are derived by the Green function method [17]:

$$\begin{aligned} \varphi(x, 0) &= \frac{\sinh(x/t)}{\sinh(L_d/t)} \times [V_d + V_1(x)] \\ &+ \frac{\sinh[(L_d - x)/t]}{\sinh(L_d/t)} V_2(x) \end{aligned} \quad (11)$$

$$\begin{aligned} E(x, 0) &= \frac{\cosh(x/t)}{\sinh(L_d/t)} \times \frac{V_d + V_1(x)}{t} \\ &- \frac{\cosh[(L_d - x)/t]}{\sinh(L_d/t)} \times \frac{V_2(x)}{t} \end{aligned} \quad (12)$$

where  $V_1(x) = \frac{1}{t} \int_x^{L_d} \sinh[(L_d - x)/t] V_0(x) dx$  and  $V_2(x) = \frac{1}{t} \int_0^x \sinh(x/t) V_0(x) dx$ . Eq. (11) and (12) are unified models to depict the potential and electric field of the device with an arbitrary doping profile. When the drift region is partially depleted,  $L_d$  in Eq. (11)-(12) is replaced by the lateral depletion width  $w_{lat}$ , which can be obtained by solving  $E(w_{lat}, 0) = 0$ . When a gate overlap is considered in the structure, the influence of the gate overlap on the potential and electric fields can be replaced by an effective concentration based on the theory presented in [15]. In this case,  $N(x, y)$  in Eq. (11)-(12) is replaced by an effective doping profile  $N_{eff}(x, y)$  which is obtained by adding  $N(x, y)$  to an additional effective concentration  $N_g(x)$ .  $N_g(x)$  represents the influence of the gate overlap, which is yielded by

$$N_g(x) = \begin{cases} \frac{(\epsilon_{ox} t_s + \epsilon_{ox}^2 t_{ox} / \epsilon_s) (V_{gs} - V_{FB})}{q t_{fox} l^2}, & 0 \leq x \leq L_{g'} \\ 0, & L_{g'} < x \leq L_d \end{cases} \quad (13)$$

where  $V_g$  is the applied gate voltage,  $V_{FB}$  is the flat band voltage,  $t_{fox}$  is the thicknesses of the gate oxide layer and  $L_{g'}$  represents the length of gate overlap above the drift region [15].

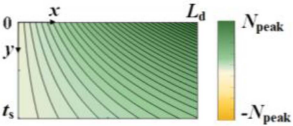
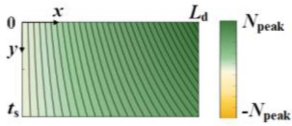
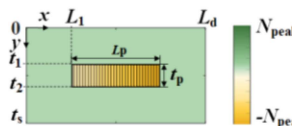
## B. CONTINUOUS DOPING PROFILE

To analyse the effect of a non-uniform drift doping profile, the surface electric fields of devices with continuous doping profiles are investigated, including a Lateral Linear and Vertical Gaussian (LLVG) doping profile, and a Lateral Linear and Vertical Linear (LLVL) doping profile. The simulation results are obtained from MEDICI. Table 1 lists expressions and schematics of the drift doping profile in the analysed lateral power device with continuous doping profiles. The drift doping profile of the analyzed device is defined by:

$$N(x, y) = N_0 + N_D \alpha(x) \beta(y) \quad (14)$$

where  $N_0$  represents the doping concentration of silicon and  $N_D$  is the initial doping concentration of the VLD layer.  $\alpha(x)$  and  $\beta(y)$  represent the variation of doping concentration in the  $x$  and  $y$  directions, respectively. According to the expression of  $N(x, y)$  and Eq. (11)-(12), the surface potential and electric field of the device with the given doping profile can be obtained. In devices with a vertical Gaussian doping profile,  $\lambda$  is related to the annealing time in practical fabrication. When it tends to infinity, namely when the annealing time is infinite, the vertical doping profile is nearly uniform. In terms of the device with a vertical linear doping profile, when  $c_L/c_V$  becomes zero, the device is uniformly doped in the lateral/vertical direction. Thus, the device with a lateral/vertical uniform doped drift region is not discussed

**TABLE 1.** Parameters of doping profile of different devices in which  $N(x,y) = N_0 + N_D\alpha(x)\beta(y)$ .

Doping profile type	Continuous Doping Profile		Discrete Doping Profile
	Lateral Linear and Vertical Gaussian (LLVG)	Lateral Linear and Vertical Linear (LLVL)	Linear D/T-RESURF
Analytical expression of $\alpha(x)$	$1 + c_L \frac{x}{L_d}$	$1 + c_L \frac{x}{L_d}$	$\begin{cases} 1 - c_L \frac{x - L_1}{L_p}, x \in (L_1, L_1 + L_p) \\ 0, \text{otherwise} \end{cases}$
Analytical expression of $\beta(y)$	$e^{-\left(\frac{y}{\lambda}\right)^2}$	$1 - c_V \frac{y}{t_s}$	$\begin{cases} 1, y \in (t_1, t_2) \\ 0, \text{otherwise} \end{cases}$
Schematic of $N(x,y)$			

Notes:  $N_0$  represents the doping concentration of silicon and  $N_D$  is the initial doping concentration of the VLD layer.  $\alpha(x)$  and  $\beta(y)$  represent the variation of doping concentration in the  $x$  and  $y$  directions, respectively.  $\lambda$  is the characteristic length in Gaussian doping profile.  $c_L$  and  $c_V$  are the slopes of lateral and vertical doping profiles, respectively.  $t_s$  is the thicknesses of the drift region.  $L_1, t_1, t_2$  represent left, top and bottom location of the buried layer, respectively;  $L_p$  is length of the buried layer.

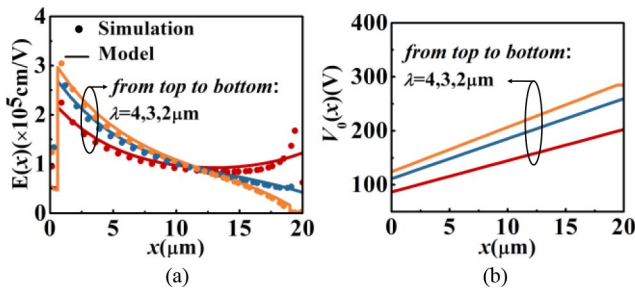


**FIGURE 3.** The device with LLVG doping profile: (a) surface electric field distributions in the drift region and (b) value of effective substrate voltage. ( $V_d = 230\text{V}$ ,  $t_s = 3\mu\text{m}$ ,  $t_{ox} = 3\mu\text{m}$ ,  $L_d = 20\mu\text{m}$ ,  $L'_g = 0.5\mu\text{m}$ ,  $c_L = 2.3$ ,  $N_0 = 1 \times 10^{12} \text{cm}^{-3}$ ,  $N_D = 3 \times 10^{15} \text{cm}^{-3}$ ).

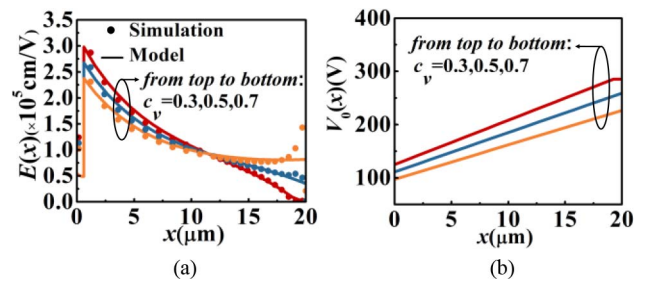


**FIGURE 4.** The device with LLVL doping profile: (a) surface electric field distributions in the drift region and (b) value of effective substrate voltage. ( $V_d = 230\text{V}$ ,  $t_s = 3\mu\text{m}$ ,  $t_{ox} = 3\mu\text{m}$ ,  $L_d = 20\mu\text{m}$ ,  $L'_g = 0.5\mu\text{m}$ ,  $c_L = 2.3$ ,  $N_0 = 1 \times 10^{12} \text{cm}^{-3}$ ,  $N_D = 3 \times 10^{15} \text{cm}^{-3}$ ).

separately. Fig. 3 and Fig. 4 illustrate the impact of doping profiles on the surface electric field and effective substrate voltage. Although these devices have the same lateral doping parameters, the surface electric field varies due to the different value of  $V_0(x)$ . According to the ESV theory, the slope of  $V_0(x)$  represents the effect of the vertical doping profile. An increased  $\lambda$  or a decreased  $c_V$  contributes to a higher value of charge  $Q$  in the differential layer, which ultimately leads to an increased  $V_0(x)$ . Thus, the slope of  $V_0(x)$  in the device with different vertical doping profile is different even though these devices have a same  $\alpha(x)$ , as shown in Fig. 3(b) and Fig. 4 (b). The high effective substrate voltage makes the drift region hard to deplete. Additionally, the effective substrate voltage represents the influence of depleted charges in the drift region, so the value of  $V_0(x)$  might be higher than  $V_d$ , as shown in Fig. 3(b) and Fig. 4 (b).

### C. DISCRETE DOPING PROFILE

The proposed analytical model can also be applied to the SOI LDMOS with a discrete arbitrary doping profile, for

example, a Double/Triple RESURF (D/T-RESURF) device. To further improve the breakdown voltage of D/T-RESURF lateral power devices, the p-type layer of the discussed devices is designed to be linear-doped. The  $N(x, y)$  of linear D/T-RESURF devices are given in Table 1. Based on the expression of in Table 1 and Eq. (11)-(12), the surface potential and electric field of each region can be obtained. When  $N_D$  and  $c_L$  are equal to 0, the doping profile in the drift region is uniform and  $V_0(x)$  can be transformed into  $V_0(x)$  of a uniformly doped device.

Fig. 5 and Fig. 6 show the surface electric field and the effective substrate voltage of the linear D-RESURF and T-RESURF lateral power devices, respectively. Different doping profiles lead to different surface electric field distributions, as shown in Fig. 5 (a) and Fig. 6(a). It is worth noting that, in the device with discrete lateral doping profile, the function of  $V_0(x)$  is also discrete. According to the Eq. (6), the basic function of  $V_0(x)$  is decided by the lateral doping profile, while the value of  $V_0(x)$  is influenced by the entire doping profile in the drift region. Therefore,

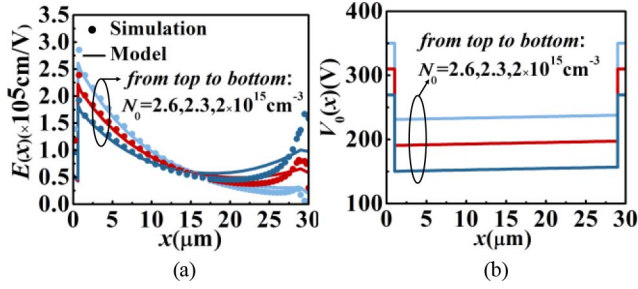


**FIGURE 5.** The linear D-RESURF device: (a) surface electric field distributions in the drift region and (b) value of effective substrate voltage. ( $V_d = 250\text{V}$ ,  $t_s = 7\mu\text{m}$ ,  $t_1 = 0\mu\text{m}$ ,  $t_2 = 1\mu\text{m}$ ,  $t_{ox} = 3\mu\text{m}$ ,  $L_d = 30\mu\text{m}$ ,  $L_p = 28\mu\text{m}$ ,  $L_1 = 1\mu\text{m}$ ,  $L'_g = 0.5\mu\text{m}$ ,  $N_D = -5 \times 10^{15}\text{cm}^{-3}$ ,  $c_L = 0.056$ ).

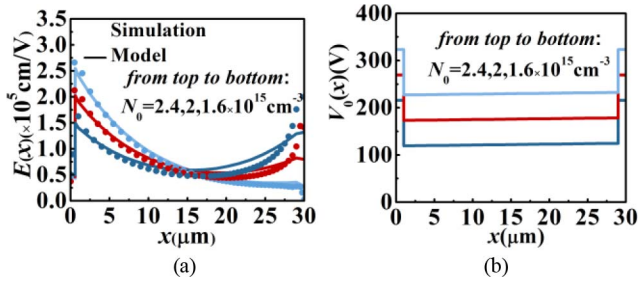


**FIGURE 6.** The linear T-RESURF device: (a) surface electric field distributions in the drift region and (b) value of effective substrate voltage. ( $V_d = 250\text{V}$ ,  $t_s = 7\mu\text{m}$ ,  $t_1 = 3\mu\text{m}$ ,  $t_2 = 4\mu\text{m}$ ,  $t_{ox} = 3\mu\text{m}$ ,  $L_d = 30\mu\text{m}$ ,  $L_p = 28\mu\text{m}$ ,  $L_1 = 1\mu\text{m}$ ,  $L'_g = 0.5\mu\text{m}$ ,  $N_D = -5 \times 10^{15}\text{cm}^{-3}$ ,  $c_L = 0.056$ ).

the impacts of lateral and vertical doping profiles could be depicted by  $V_0(x)$ . Since the partial-depletion case in discrete devices is more complex and lacks meaning in the application, it will not be explored in this paper.

### III. BREAKDOWN VOLTAGE

To investigate the breakdown mechanism of SOI LDMOS with various drift doping profiles, the breakdown model is derived. The length of gate overlap is always designed to be small in order to reduce the parasitic capacitance. Therefore, the effect of gate overlap is ignored in the analysis of breakdown voltage. The breakdown cases can be divided into lateral breakdown and vertical breakdown. Lateral breakdown always occurs at PN junction and  $N^+N$  junction when the drift region is fully depleted. When the device is partially depleted, it emerges at PN junction. Therefore, the breakdown cases are divided as follows:

1) *Lateral PN Junction Partial-Depletion Breakdown*: By submitting  $E_x(0, 0) = E_C$  into Eq. (12) in the partial depletion case, the lateral  $BV_{P,lat}^{PN}$  can be expressed as:

$$BV_{P,lat}^{PN} = E_C t \sinh(w_{lat}/t) - V_1(0) \quad (15)$$

2) *Lateral PN Junction Full-Depletion Breakdown*: The lateral  $BV_{F,lat}^{PN}$  can be obtained by substituting the boundary condition  $E_x(0, 0) = E_C$  into Eq. (12), which yields:

$$BV_{F,lat}^{PN} = E_C t \sinh(L_d/t) - V_1(0) \quad (16)$$

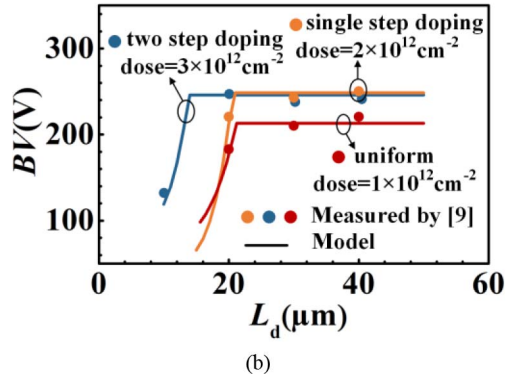
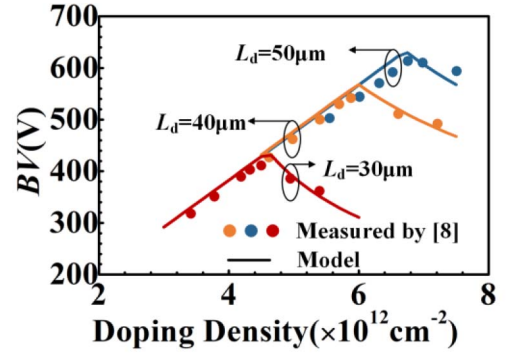


**FIGURE 7.** The measured and modeled breakdown voltage: (a) VLD device ( $t_s = 0.15\mu\text{m}$ ,  $t_{ox} = 2\mu\text{m}$ ); (b) device with step doped drift region ( $t_s = 3\mu\text{m}$ ,  $t_{ox} = 0.15\mu\text{m}$ ,  $\lambda = 10\mu\text{m}$ ).

3) *Lateral  $N^+N$  Junction Full-Depletion Breakdown*: According to the boundary condition  $E_x(L_d, 0) = E_C$  and Eq. (12), the lateral  $BV_{F,lat}^{NN}$  can be derived as:

$$BV_{F,lat}^{NN} = \frac{1}{\cosh(L_d/t)} \times [E_C t \sinh(L_d/t) + V_2(L_d)] \quad (17)$$

4) *Vertical Breakdown*: The vertical breakdown assumes to occur at point  $(L_d, t_s)$ . Based on the boundary condition  $E(L_d, t_s) = E_C$ , the vertical BV can be obtained as [6]:

$$BV_{F,ver} = E_C(t_s + \varepsilon_{ox}t_{ox}/\varepsilon_s) - \frac{q}{\varepsilon_s} \int_0^{t_s} N(L_d, y) y dy \quad (18)$$

The breakdown voltage is limited by the minimum lateral and vertical BV, so the BV of the complete structure is:

$$BV = \min[BV_{P,lat}^{PN}, BV_{F,lat}^{PN}, BV_{F,lat}^{NN}, BV_{F,ver}] \quad (19)$$

The measured and modeled breakdown voltage of the device with different doping profiles are compared in Fig. 7. Fig. 7(a) gives BV of the VLD device and Fig. 7(b) illustrates BV of the device with lateral step doped and vertical Gaussian doped drift region. The good agreement verifies the correction of the derived model. In order to further investigate the impact of doping profile on BV, MEDICI is used here to obtain BV under more situations. The breakdown voltages of the devices with LLVG and LLVL doping profile are shown in Fig. 8. It is obvious that the maximum breakdown is unchanged for different vertical

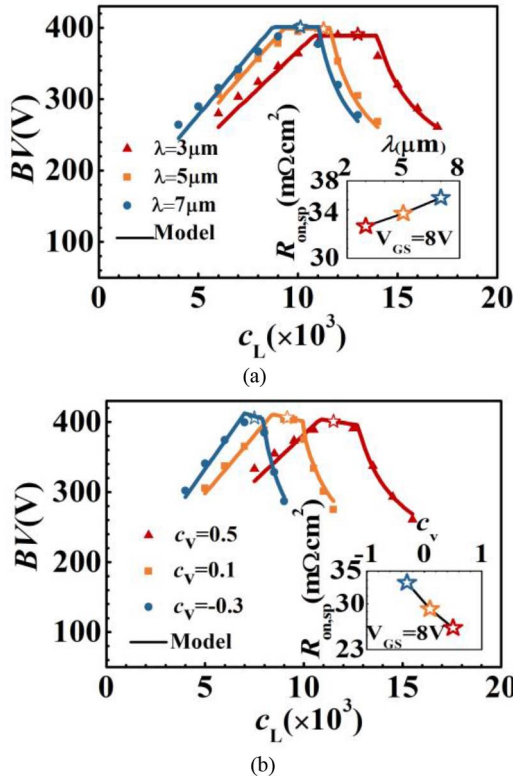


**FIGURE 8.** Breakdown voltage of (a) the device with LLVG doping profile and (b) the device with LLVL doping profile. ( $N_0 = N_D = 1 \times 10^{12}\text{cm}^{-3}$ ,  $t_s = 3\mu\text{m}$ ,  $t_{\text{ox}} = 3\mu\text{m}$ ,  $L_d = 20\mu\text{m}$ ).

parameters, including  $\lambda$  and  $c_v$ . In contrast, the related optimal lateral doping parameter shifts with the variation of  $\lambda$  or  $c_v$ . As shown in the sub-plot of Fig. 8, devices with small  $\lambda$  or large  $c_v$  have a larger optimal  $c_L$ , leading to a reduced on-resistance. simulation results, which reveals that this breakdown model can be applied in the device with discrete doping profile. It also illustrates that devices with a large absolute value of  $N_D$  have an increased optimal  $N_0$ , which is marked as a star symbol. The sub-plot in Fig. 9 reveals that the increased  $N_0$  results in a small Fig. 9 illustrates the breakdown voltage of the linear D/T-RESURF device. The analytical results agree well with the on-resistance. Moreover, it is desirable that BV of the device with a large absolute value of  $N_D$  changes little near the point of optimal  $N_0$ , which shows a better characteristic of process tolerance.

#### IV. RESURF CRITERION

The RESURF criterion is an important issue in maximizing the breakdown voltage and guiding the design of lateral power devices. To obtain an idealized electric field, we assume that  $E(0,0) = E(L_d,0)$  and that the doping profile satisfies the following equation:

$$E_C t \sinh(L_d/t) [\cosh(L_d/t) - 1] = \cosh(L_d/t) V_1(0) + V_2(L_d) \quad (20)$$

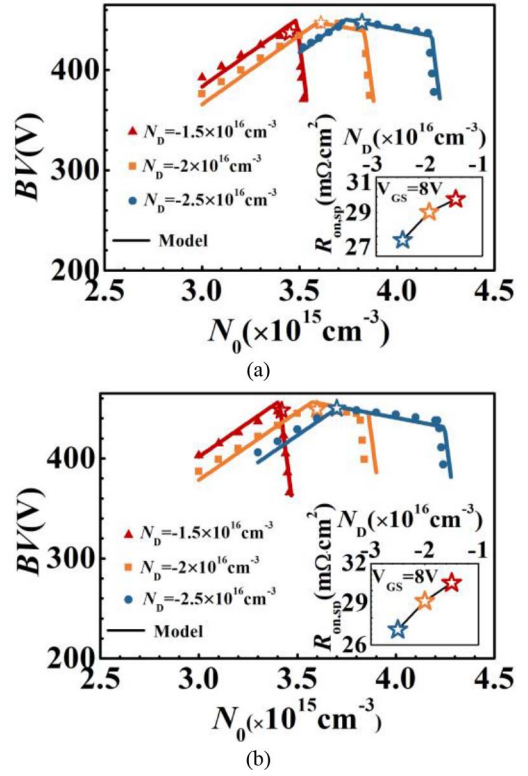


**FIGURE 9.** Breakdown voltage of (a) linear D-RESURF device ( $t_1 = 0\mu\text{m}$ ,  $t_2 = 1\mu\text{m}$ ) and (b) linear T-RESURF device ( $t_1 = 3\mu\text{m}$ ,  $t_2 = 4\mu\text{m}$ ). ( $t_s = 7\mu\text{m}$ ,  $t_{\text{ox}} = 3\mu\text{m}$ ,  $L_p = 28\mu\text{m}$ ,  $L_d = 30\mu\text{m}$ ).

In this case, the related breakdown voltage can be obtained by equating Eq. (16) and (17), yielding:

$$BV_{\text{lat}} = \frac{2}{t \sinh(L_d/2t)} \int_0^{L_d} \cosh[(L_d/2 - x)/t] V_0(x) dx \quad (21)$$

Based on Eq. (20) and (21), a RESURF criterion and a maxim  $BV_{\text{lat}}$  of the device with an arbitrary doping profile are obtained. When the drift region is uniformly doped, the RESURF criterion and the related lateral breakdown voltage of the conventional S-RESURF can be obtained as:

$$D(x) = \frac{\varepsilon_s E_C}{q} \tanh(L_d/2t) \quad (22)$$

$$BV_{\text{lat}} = 2E_C t \tanh(L_d/2t) \quad (23)$$

where  $D(x) = N_d(x) \times t$  represents the dose of the device. These equations indicate that when  $L_d \gg 2t$ ,  $BV_{\text{lat}} \approx 2E_C t$  is the maximum value of the breakdown voltage for the S-RESURF device.

#### A. CONTINUOUS DOPING PROFILE

For devices with continuous doping profiles, the vertical doping profile has a strong impact on BV. However, the conventional design of VLD power devices always assumes the vertical doping profile to be uniform. In practical fabrication, after a typical annealing process (lasting 960min at  $1150^\circ\text{C}$ ) for forming the drift region [7], the vertical doping profile

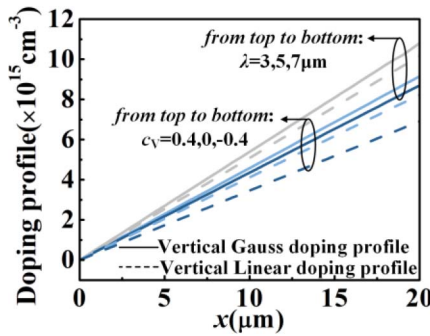


**FIGURE 10.** Optimal doping profile of device with continuous doping profile ( $t_s = 3\mu\text{m}$ ,  $t_{ox} = 3\mu\text{m}$ ,  $L_d = 20\mu\text{m}$ ).

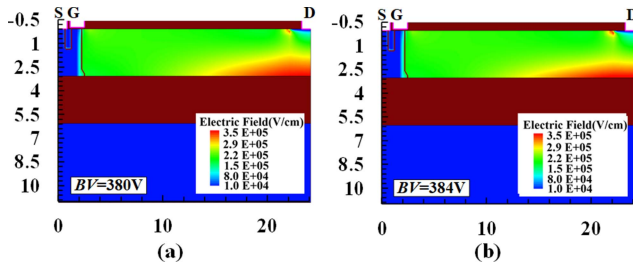


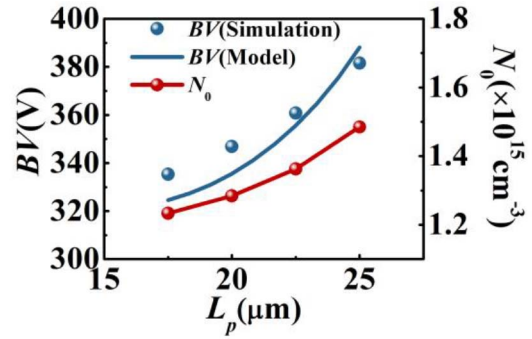
**FIGURE 11.** Electric field distribution at breakdown of (a) device with optimal LLVG doping profile ( $\lambda = 5\mu\text{m}$ ,  $t_s = 3\mu\text{m}$ ,  $t_{ox} = 3\mu\text{m}$ ,  $L_d = 20\mu\text{m}$ ); (b) device with optimal LLV doping profile ( $c_V = -0.4$ ,  $t_s = 3\mu\text{m}$ ,  $t_{ox} = 3\mu\text{m}$ ,  $L_d = 20\mu\text{m}$ ).

in the drift region is Gaussian, and  $\lambda$  is approximately  $7\mu\text{m}$ . For the specific geometric parameters of the lateral power device used in Fig. 7, the optimal  $c_L$  of the conventional VLD device is  $8 \times 10^3$ , and the BV is 401V when the vertical doping profile is uniform. If the practical situation is considered, the BV of this conventional VLD device will decrease by 8.7% (from 401 V to 366 V) according to Fig. 8.

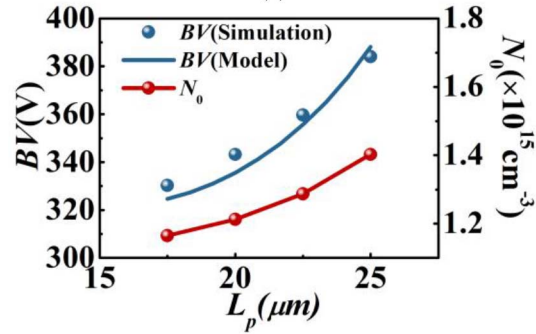
To prohibit the degradation of BV and obtain a maximum BV in a device with a different vertical doping profile, the surface electric field is assumed to be uniform, and  $E_x(x, 0) = E_C$  is substituted into Eq. (10), and the RESURF criterion of the device with a continuous doping profile can be obtained as:

$$D(x) = \frac{N_D E_C t}{V_0(0)} x \quad (24)$$

This value also satisfies Eq. (20). When the vertical doping profile is uniform, Eq. (24) tends to the case of an ideal VLD profile [4], [12]. The optimal doping profile based on Eq. (24) is shown in Fig. 10. The profiles indicate that small  $\lambda$  or large  $c_V$  leads to a large doping profile at the surface of the drift region. Fig. 11 shows the distribution of the electric field at breakdown in the device with an optimal doping profile based on Eq. (24) and Fig. 10. Further, the distribution reveals that the surface electric field remains to be uniform and the breakdown voltage is almost unchanged.



(a)



(b)

**FIGURE 12.** Breakdown voltage at different  $L_p$  in (a) D-RESURF; (b) T-RESURF device ( $t_s = 7\mu\text{m}$ ,  $t_{ox} = 3\mu\text{m}$ ,  $L_d = 30\mu\text{m}$ ).

## B. DISCRETE DOPING PROFILE

In addition to the geometric structure of the VLD layer, the doping concentration outside the buried layer in discrete devices is also vital, because it determines electric field peaks at both ends of the drift region. In terms of D/T RESURF devices, the length of  $L_1$  is always designed to be very small in order to gain a high breakdown voltage. The RESURF criterion of D/T RESURF devices can also be obtained by substituting Eq. (20) into Eq. (24), which yields:

$$D(x) \approx \frac{\epsilon_s E_C}{q} \times \frac{L_d}{L_p(L_d - L_p)/2t + 2t} \quad (25)$$

In addition, the maximized breakdown voltage of the D/T RESURF device can be gained by combining Eq. (24) and Eq. (25) into Eq. (21), given as:

$$BV_{lat} \approx 2E_C t \times \frac{L_d}{L_p(L_d - L_p)/2t + 2t} \quad (26)$$

When the buried layer disappears in the drift region, namely,  $L_p = 0$ , the device becomes a S-RESURF device and Eq. (25)-(26) become Eq. (22)-(23). To obtain a device with a higher breakdown voltage than the conventional S-RESURF device,  $L_p$  should be greater than  $2t$  based on Eq. (26). Obviously, the  $BV_{lat}$  and  $N_D$  increase with  $L_p$  according to Eq. (25)-(26), which is also shown in Fig. 12. Thus, the  $L_p$  should be designed to be sufficiently large. Due to the assumption of a small  $L_1$ , the model is not very accurate at small  $L_p$ . It is also worth noting that when  $L_p = L_d$ ,  $BV_{lat} = E_C L_d$  based on Eq. (26), which reveals

that the lateral electric field could become uniform and the lateral breakdown voltage is maximized in the device with a sufficiently long buried layer.

## V. CONCLUSION

By using the proposed ESV method, the relationship between 2-D arbitrary doping profile of the drift region and SOI LDMOS' off-state breakdown characteristic is analytically explored. The veracity and efficiency of the proposed methodology are well verified by the good agreement between analytical, experimental and simulated results. In particular, the lateral power devices with different drift region doping types, such as LLVG/LLVL and the linear D/T-RESURF are demonstrated and discussed in detail. Furthermore, by using the proposed model, a generally applicable RESURF criterion is given to optimize the doping profiles and geometric parameters. According to this RESURF criterion, a uniform surface electric field can be obtained only in devices with continuous drift doping profiles. Meanwhile, in terms of devices with discrete drift region doping, a maximum lateral BV can be achieved with a properly designed buried layer. The obtained RESURF criterion can be combined with other parameters to give guidance for the optimal design of lateral power devices with arbitrary doping profile.

## REFERENCES

- [1] M. Qiao *et al.*, "3-D edge termination design and  $R_{ON,sp}$ -BV model of a 700-V triple RESURF LDMOS with N-type top layer," *IEEE Trans. Electron Devices*, vol. 64, no. 6, pp. 2579–2586, Jun. 2017, doi: [10.1109/LED.2017.2694451](https://doi.org/10.1109/LED.2017.2694451).
- [2] W. W. Ge *et al.*, "Ultra-low ON-resistance LDMOS with multi-plane electron accumulation layer," *IEEE Electron Device Lett.*, vol. 38, no. 7, pp. 910–913, Jul. 2017, doi: [10.1109/LED.2017.2701354](https://doi.org/10.1109/LED.2017.2701354).
- [3] Y. F. Guo, J. F. Yao, B. Zhang, H. Lin, and C. C. Zhang, "Variation of lateral width technique in SOI high-voltage lateral double-diffused metal-oxide-semiconductor transistors using high-k dielectric," *IEEE Electron Device Lett.*, vol. 36, no. 3, pp. 262–264, Mar. 2015, doi: [10.1109/LED.2015.2393913](https://doi.org/10.1109/LED.2015.2393913).
- [4] J. Zhang, Y.-F. Guo, D. Z. Pan, K.-M. Yang, X.-J. Lian, and J.-F. Yao, "Effective doping concentration theory: A new physical insight for the double-RESURF lateral power devices on SOI substrate," *IEEE Trans. Electron Devices*, vol. 65, no. 2, pp. 648–654, Feb. 2018, doi: [10.1109/LED.2017.2786139](https://doi.org/10.1109/LED.2017.2786139).
- [5] K. M. Yang *et al.*, "A novel variation of lateral doping technique in SOI LDMOS with circular layout," *IEEE Trans. Electron Devices*, vol. 65, no. 4, pp. 1447–1452, Apr. 2018, doi: [10.1109/LED.2018.2808193](https://doi.org/10.1109/LED.2018.2808193).
- [6] T.-T. Hua, Y.-F. Guo, Y. Yu, S. Gene, T. Jian, and J. F. Yao, "Analytical models of lateral power devices with arbitrary vertical doping profiles in the drift region," *Chin. Phys. B*, vol. 22, no. 5, pp. 1–9, 2013, doi: [10.1088/1674-1056/22/5/058501](https://doi.org/10.1088/1674-1056/22/5/058501).
- [7] S. Hardikar, R. Tadikonda, D. W. Green, K. V. Vershinin, and E. M. S. Narayanan, "Realizing high-voltage junction isolated LDMOS transistors with variation in lateral doping," *IEEE Trans. Electron Devices*, vol. 51, no. 12, pp. 2223–2228, Dec. 2004, doi: [10.1109/LED.2004.839104](https://doi.org/10.1109/LED.2004.839104).
- [8] S. Zhang, J. K. O. Sin, T. M. L. Lai, and P. K. Ko, "Numerical modeling of linear doping profiles for high-voltage thin-film SOI devices," *IEEE Trans. Electron Devices*, vol. 46, no. 5, pp. 1036–1041, May 1999, doi: [10.1109/16.760414](https://doi.org/10.1109/16.760414).
- [9] Y. F. Guo, Z. J. Li, and B. Zhang, "Design and fabrication of a high performance LDMOSFET with step doped drift region on bonded SOI wafers," in *Proc. Int. Conf. Commun. Circuits Syst. (ICCCAS)*, Guilin, China, 2006, pp. 2741–2744, doi: [10.1109/ICCCAS.2006.285236](https://doi.org/10.1109/ICCCAS.2006.285236).
- [10] E. Lampin, E. Dubois, H. Xu, S. Bardy, and F. Murray, "Accurate modeling of large angle tilt and pure vertical implantations: Application to the simulation of n- and p-LDMOS backgates," *IEEE Trans. Electron Devices*, vol. 50, no. 5, pp. 1401–1404, May 2003, doi: [10.1109/LED.2003.813464](https://doi.org/10.1109/LED.2003.813464).
- [11] Z. M. Dong, B. X. Duan, C. Fu, H. J. Guo, Z. Cao, and Y. T. Yang, "Novel LDMOS optimizing lateral and vertical electric field to improve breakdown voltage by multi-ring technology," *IEEE Electron Device Lett.*, vol. 39, no. 9, pp. 1358–1361, Sep. 2018, doi: [10.1109/LED.2018.2854417](https://doi.org/10.1109/LED.2018.2854417).
- [12] S. Merchant, E. Arnold, H. Baumgart, S. Mukherjee, H. Pein, and R. Pinker, "Realization of high breakdown voltage (>700V) in thin SOI devices," in *Proc. Int. Symp. Power Semicond. Devices ICs (ISPSD)*, Baltimore, MD, USA, 1991, pp. 31–35, doi: [10.1109/ISPSD.1991.146060](https://doi.org/10.1109/ISPSD.1991.146060).
- [13] Z. J. Wang *et al.*, "Realization of 850 V breakdown voltage LDMOS on Simbond SOI," *Microelectron. Eng.*, vol. 91, no. 3, pp. 102–105, 2012, doi: [10.1016/j.mee.2011.10.014](https://doi.org/10.1016/j.mee.2011.10.014).
- [14] J. Zhang, Y.-F. Guo, and D. Z. Pan, "Role of shape factor in forming surface electric field basin in RESURF lateral power devices and its optimization design," *IEEE J. Electron Devices Soc.*, vol. 6, pp. 1147–1153, Sep. 2018, doi: [10.1109/JEDS.2018.2871505](https://doi.org/10.1109/JEDS.2018.2871505).
- [15] J. Zhang, Y.-F. Guo, and D. Z. Pan, "Effective concentration profile: Mechanism of gate field-plate assistant effect in SOI lateral power devices," *IEEE Trans. Electron Devices*, vol. 65, no. 10, pp. 4476–4482, Oct. 2018, doi: [10.1109/LED.2018.2866393](https://doi.org/10.1109/LED.2018.2866393).
- [16] S.-K. Chuang, "An analytical model for breakdown voltage of surface implanted SOI RESURF LDMOS," *IEEE Trans. Electron Devices*, vol. 47, no. 5, pp. 1006–1009, May 2000, doi: [10.1109/16.841233](https://doi.org/10.1109/16.841233).
- [17] Y. F. Guo, Z. J. Li, and B. Zhang, "A new analytical model for optimizing SOI LDMOS with step doped drift region," *Microelectron. J.*, vol. 37, no. 9, pp. 861–866, 2006, doi: [10.1016/j.mejo.2006.03.004](https://doi.org/10.1016/j.mejo.2006.03.004).
- [18] P.-S. Lin and C.-Y. Wu, "A new approach to analytically solving the two-dimensional Poisson's equation and its application in short-channel MOSFET modeling," *IEEE Trans. Electron Devices*, vol. ED-34, no. 9, pp. 1947–1956, Sep. 1987, doi: [10.1109/T-ED.1987.23180](https://doi.org/10.1109/T-ED.1987.23180).
- [19] A. Nandi, N. Pandey, and S. Dasgupta, "Analytical modeling of DG-MOSFET in subthreshold regime by green's function approach," *IEEE Trans. Electron Devices*, vol. 64, no. 8, pp. 3056–3062, Aug. 2017, doi: [10.1109/LED.2017.2708603](https://doi.org/10.1109/LED.2017.2708603).
- [20] N. Pandey, H.-H. Lin, A. Nandi, and Y. Taur, "Modeling of short-channel effects in DG MOSFETs: Green's function method versus scale length model," *IEEE Trans. Electron Devices*, vol. 65, no. 8, pp. 3112–3119, Aug. 2018, doi: [10.1109/LED.2018.2845875](https://doi.org/10.1109/LED.2018.2845875).